Monte Carlo Simulation

Pravata Mohanty
TIFR, Mumbai

Cosmic Neutrino Observation at Ultra High Energies
16-23 December 2019, IIT Kanpur

Stanislaw Ulam, Enrico Fermi, John von Neumann, and Nicholas Metropolis, among others who were involved in the Manhattan project and used Monte Carlo simulation to design the first nuclear bomb during World War II.

The name is a reference to the Monte Carlo Casino where Ulam's uncle would borrow money to gamble. The use of randomness and the repetitive nature of the process are analogous to the activities conducted at a casino.

Monte Carlo method is used in almost every field of science, mathematics to economics and computer games.

Monte Carlo methods are very important in computational physics, physical chemistry, and related applied fields, and have diverse applications from complicated quantum chromodynamics calculations to designing heat shields and aerodynamic forms.

In experimental high energy and astroparticle physics, these methods are used for designing detectors, understanding their behavior and comparing experimental data to theory.

Where to use Monte Carlo

Definiteness

$$v = v_0 + a\,t$$

Randomness

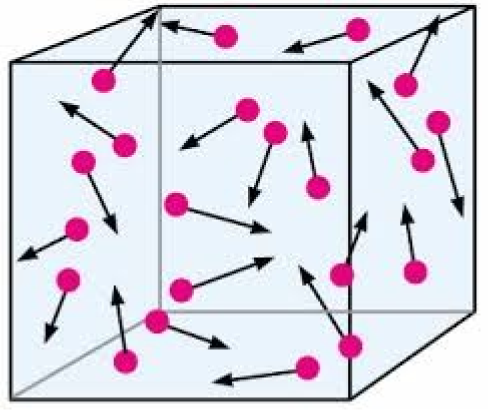

Random Numbers

Engine of Monte Carlo

99, 16, 28, 94, 23, 48, 95, 74, 54, 73

Clasification of Random Numbers

Natural or True Random Numbers

Obtained from a natural process

Examples: Muon Decay

Thermal Noise

You can store them and use

Clasification of Random Numbers

Pseudo Random Numbers

Generated by computers using some algorithm

Linear Congruential Generator

The generator is defined by the recurrence relation:

$$X_{n+1} \equiv (aX_n + c) \pmod m$$

where X_n is the sequence of pseudorandom values, and

$m,\ 0 < m$ — the "modulus"
$a,\ 0 < a < m$ — the "multiplier"
$c,\ 0 \le c < m$ — the "increment"
$X_0,\ 0 \le X_0 < m$ — the "seed" or "start value"

Linear Congruential Generator

$$\boxed{X_{n+1} \equiv (aX_n + c) \pmod{m}}$$

Example: $X_0 = 2$; $a=5$; $c=1$; $m=7$

Period length

The period of a general LCG is at most m, and for some choices of a much less than that. Provided that c is nonzero, the LCG will have a full period for all seed values if and only if:[2]

1. c and m are relatively prime,
2. $a - 1$ is divisible by all prime factors of m,
3. $a - 1$ is a multiple of 4 if m is a multiple of 4.

Source	***m***	***a***	***c***
Numerical Recipes	2^{32}	1664525	1013904223
Borland C/C++	2^{32}	22695477	1
glibc (used by GCC)[5]	2^{31}	1103515245	12345

Random Number Generators

In C/C++: rand( )

In Fortran 77 : RANDOM( )

```
for ( int i=0;  i<100;  i++) {
    int r = rand();
}
```

Uniform Random Numbers

Using C/C++ : Double r=rand()/RAND_MAX

RAND_MAX = period,

Uniform random numbers between 0 and 1 can be used

as basis to generate any random number

Muon Decay

$$\mu^- \rightarrow e^- + \nu_e + \nu_\mu$$

$dN/dt \propto N$

$N(t) = N(0)\, e^{-t/\tau}$, τ = Mean Life Time

Decay probability

$$P = \frac{\int_0^t dN/dt \,.\, dt}{\int_0^\infty dN/dt \,.\, dt} = 1 - e^{-t/\tau}$$

Continued ....

$$\boxed{t = -\tau \ln(1 - P)}$$

$$P \equiv R$$

R is Uniform Random Number between 0 and 1

Muon Decay Distribution

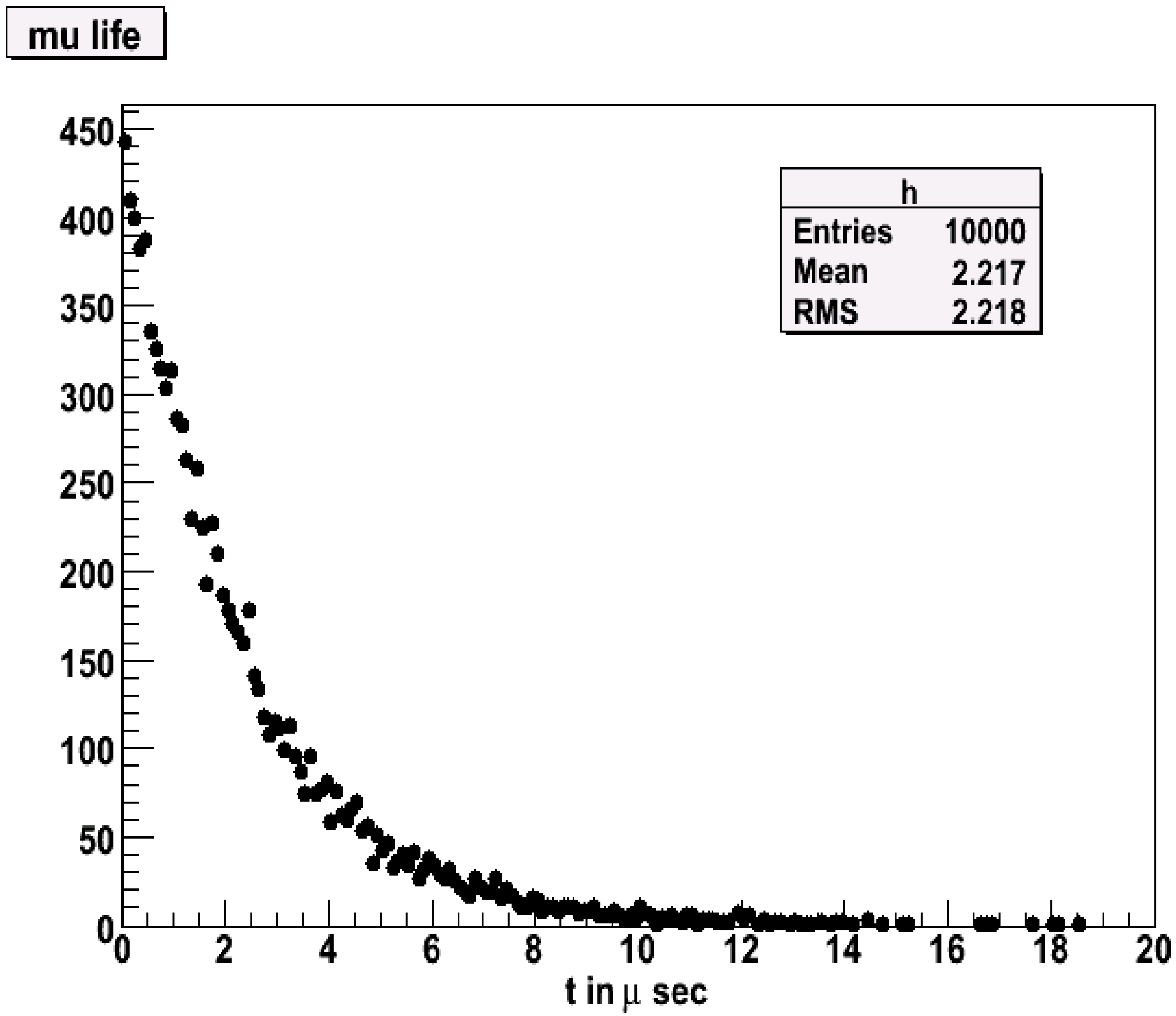

AN EXAMPLE APPLICATION

Many questions ?

- Why 2 cm not 1 cm or 3 cm or any other thickness?

- Why straight groove not some other groove ?

- Why 18 fibers in 12 grooves?

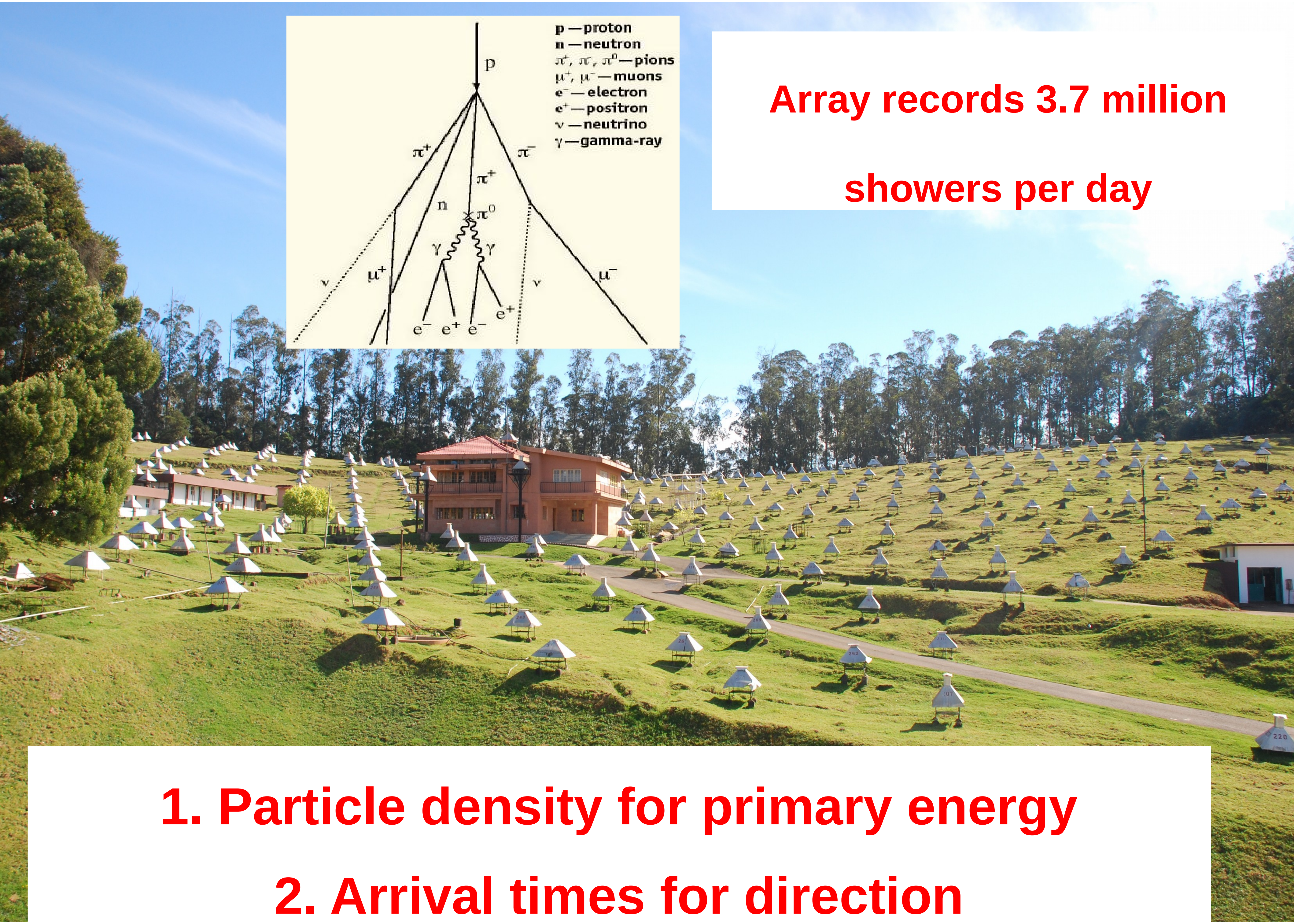

Array records 3.7 million showers per day

1. Particle density for primary energy

2. Arrival times for direction

Old scintillator detector type

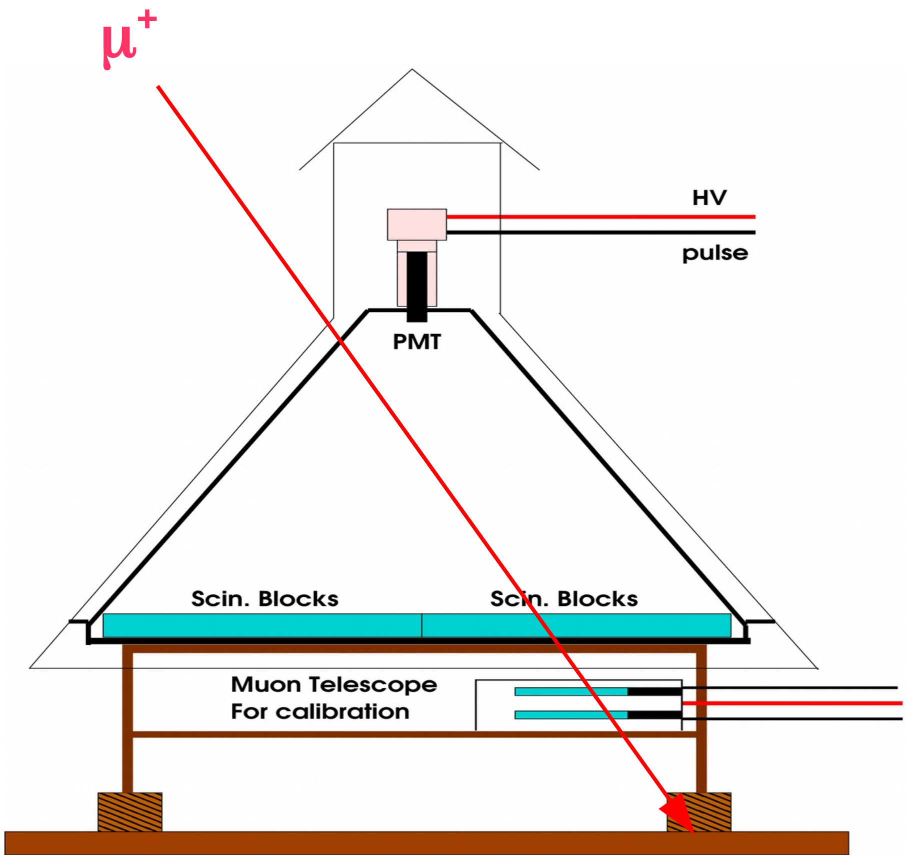

Low Photo-electron Yield (Poor Signal to Noise Separation)

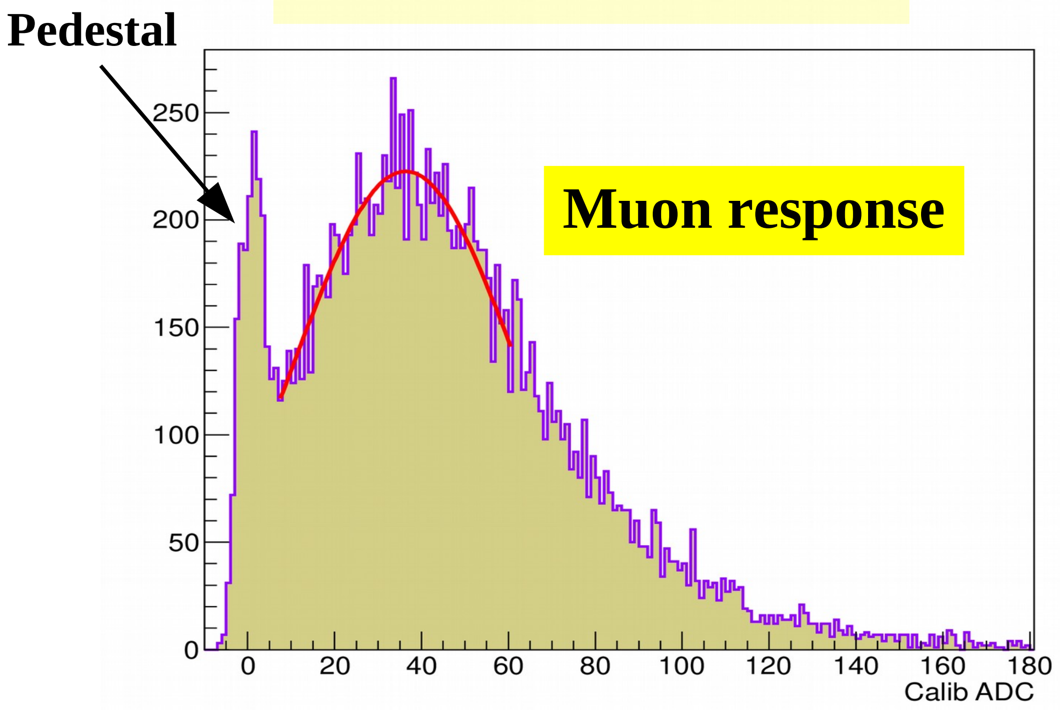

Large Non-uniform Response (~ 30%)

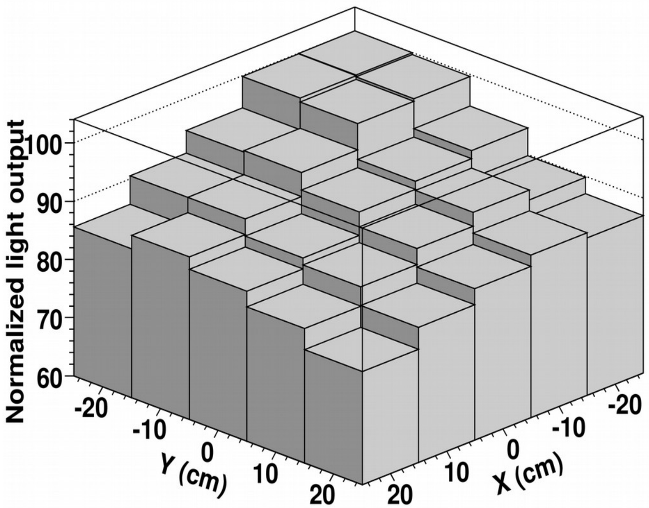

DESIGN A BETTER DETECTOR

What are Design Goals?

- **Photon yield**
- **Uniformity**
- **Timing**
- **Cost Effectiveness**
- **Ease of fabrication**

Why straight groove not some other?

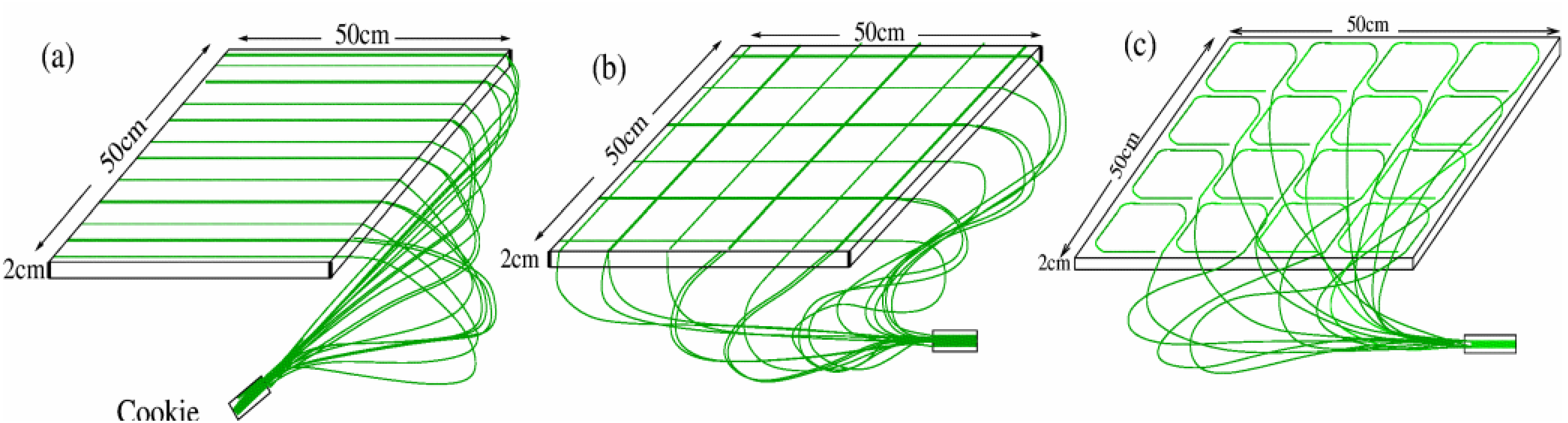

New design using WLS fibers

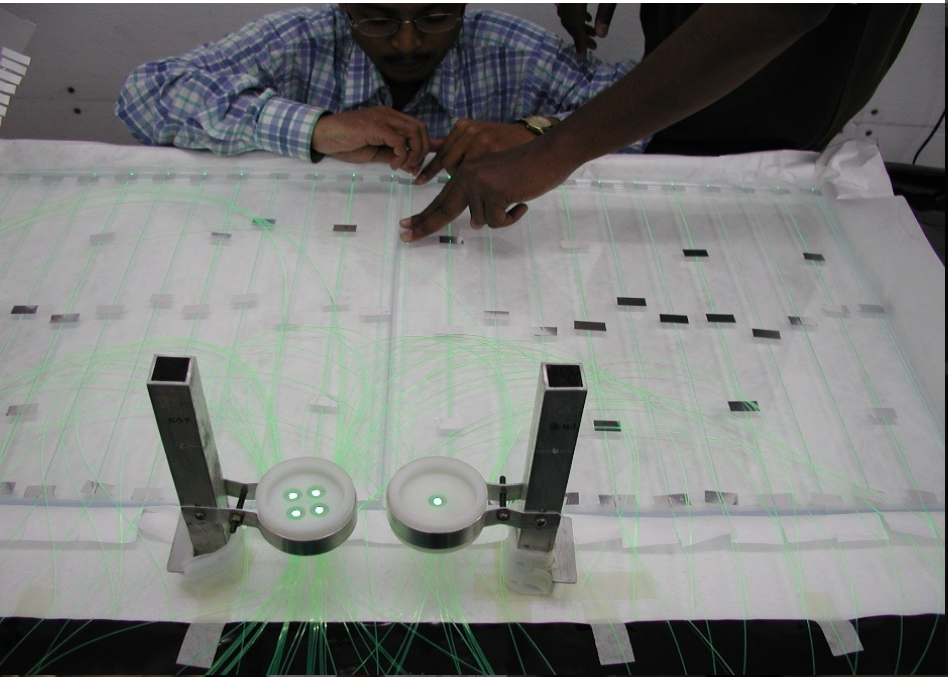

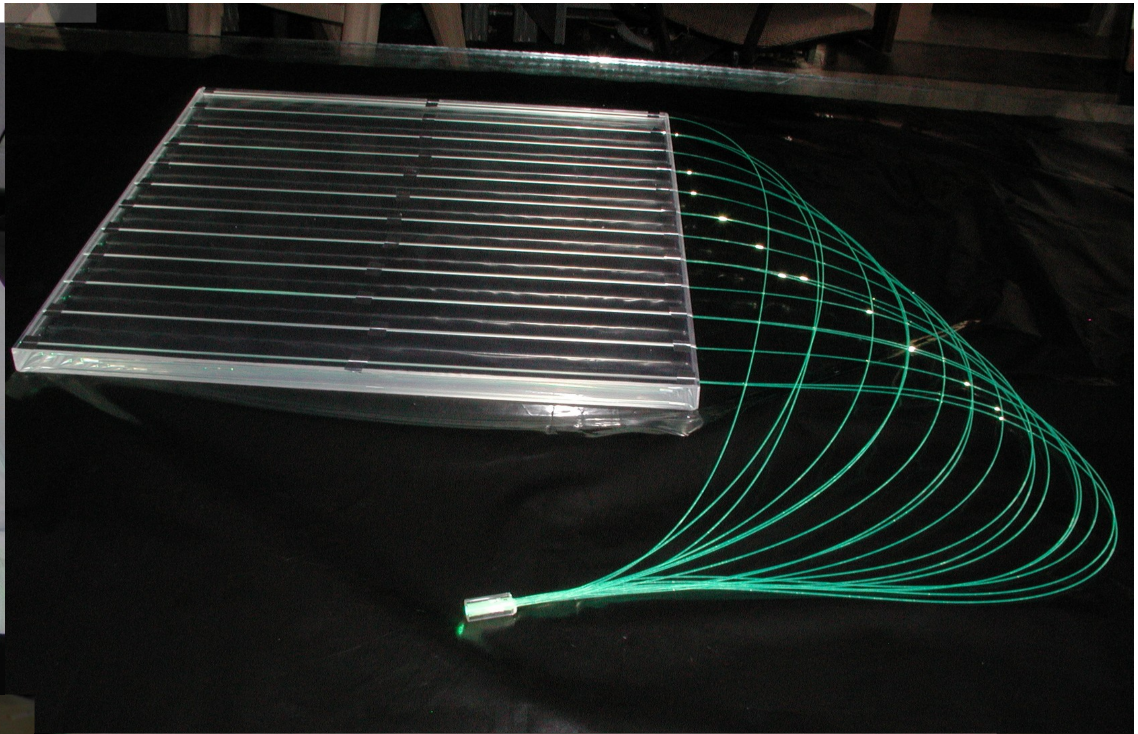

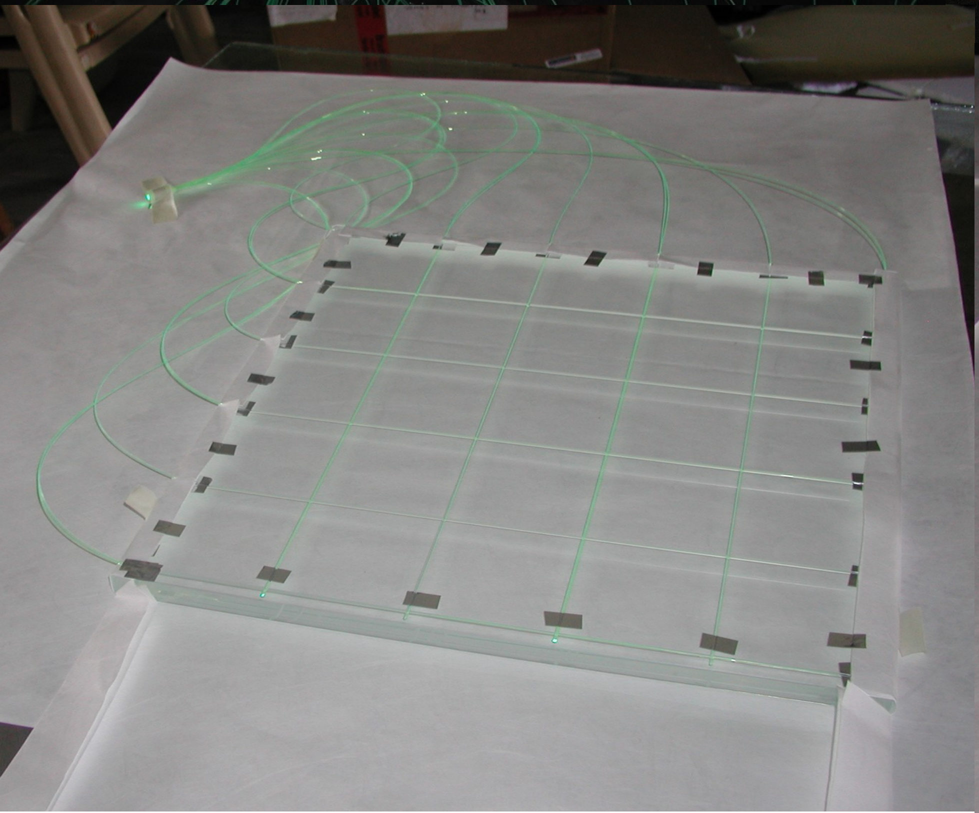

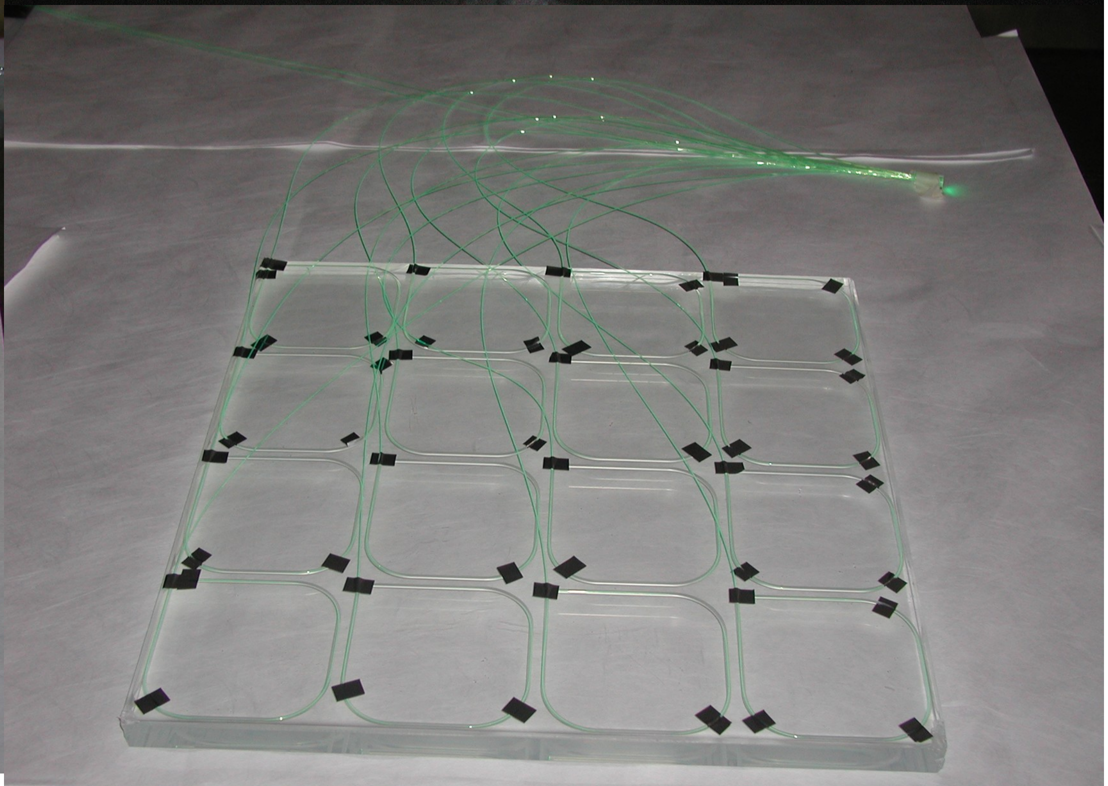

More than 20 prototypes were constructed with different groove designs, different scintillator thickness, varying number of fibers, different layers of reflectors etc.

Fabricating a prototype, testing and analysing collected data required more than two weeks.

No convergence to an optimal design after two years of effort.

Motivation for G3sim

G3sim code was developed to optimize the design of GRAPES-3 scintillator detector.

G3sim stands for GRAPES-3 simulation for scintillator detectors.

G3sim Model

1: Generation and propagation of muons

$$\frac{dN_\mu}{d\Omega} \propto \cos^2\theta.$$

2: Energy loss (dE/dX) calculation using Landau distribution

3: Generation of photons in scintillator.

4: Propagation of photons in scintillator using basic laws of reflection and considering attenuation loss and loss due to imperfect surface

5: Capture, trapping and propagation of photons in WLS fiber considering meridional and skew ray modes

6: Convolution of PMT responses.

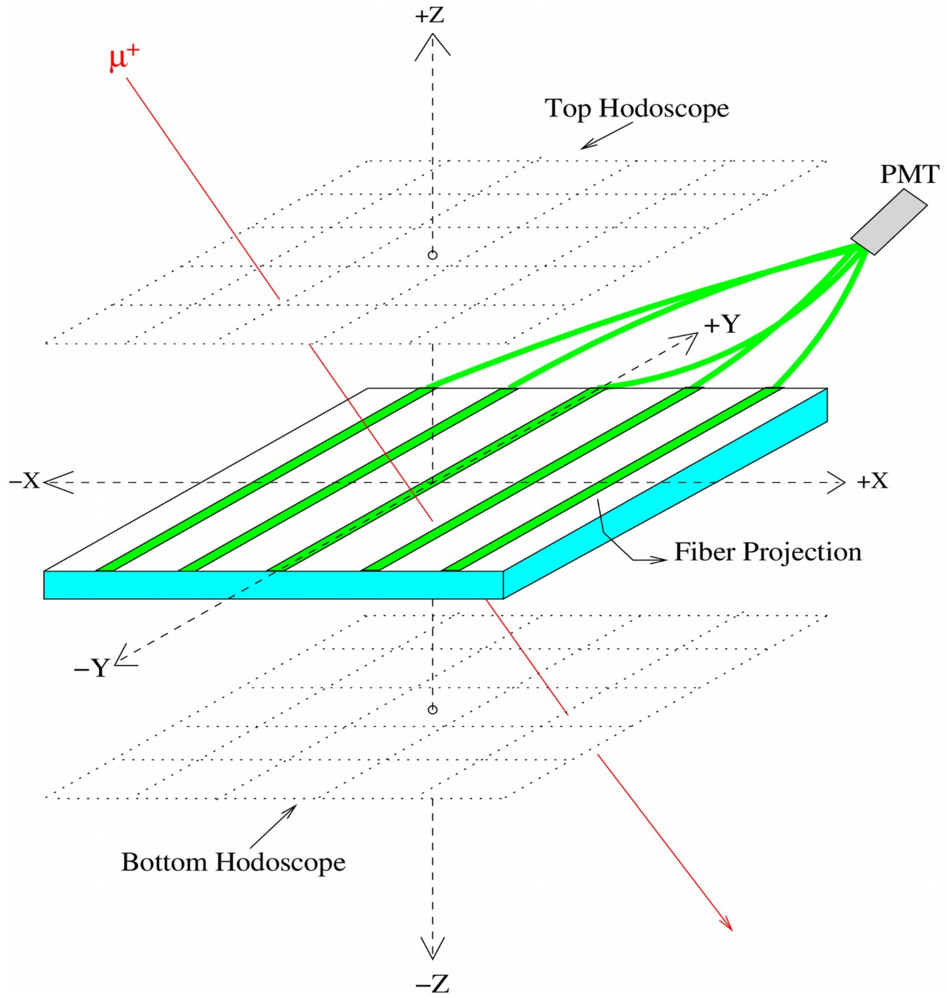

Probability distributions and uniform random numbers (0 to 1) used to model each process as the trigger. In simulations the muons are distributed uniformly on the top hodoscope using two random numbers. The simulated muon direction is distributed in zenith angle θ with a $\cos^2\theta$ dependence and uniform azimuthal angle ϕ as shown below[17,18]

$$\frac{dN_\mu}{d\Omega} \propto \cos^2\theta. \tag{1}$$

Here Ω is solid angle and $\mathrm{d}\Omega = \sin\theta d\theta d\phi$. Thus, the probability of a muon between 0 to θ is obtained by integrating Eq. (1),

$$P = \frac{\int_0^{2\pi}\int_0^{\theta}\cos^2\theta\cos\theta\sin\theta d\theta d\phi}{\int_0^{2\pi}\int_0^{60^o}\cos^2\theta\cos\theta\sin\theta d\theta d\phi}. \tag{2}$$

The muon flux was normalized for θ between 0° and 60° since the probability of muons above 60° was relatively small. Solution of Eq. (2) yields

$$\theta = \cos^{-1}((1 - 0.9375P)^{1/4}). \tag{3}$$

Here P is a random number and ϕ is randomly distributed from 0 to 2π. The location and direction of each muon through the detector is stored for further analysis. Since

Specific Energy Loss Distribution

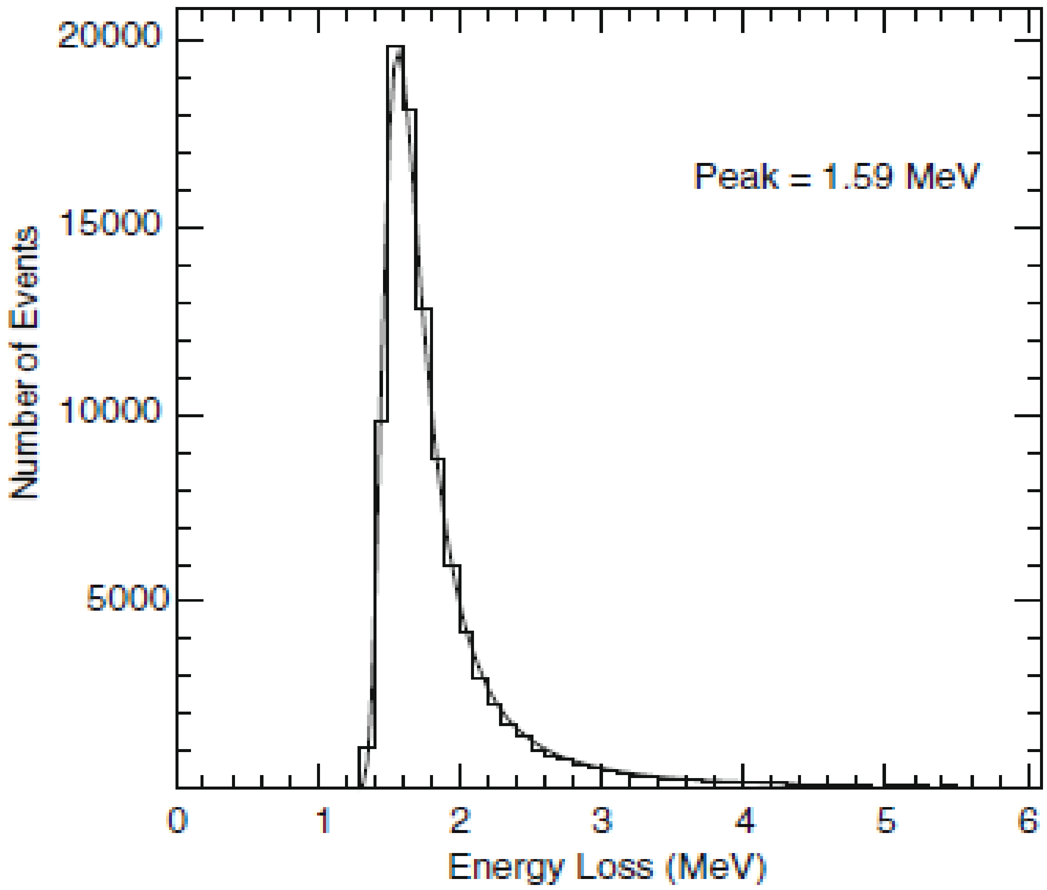

Computed Using ROOT Library function LandauI

Integral Probability Distribution

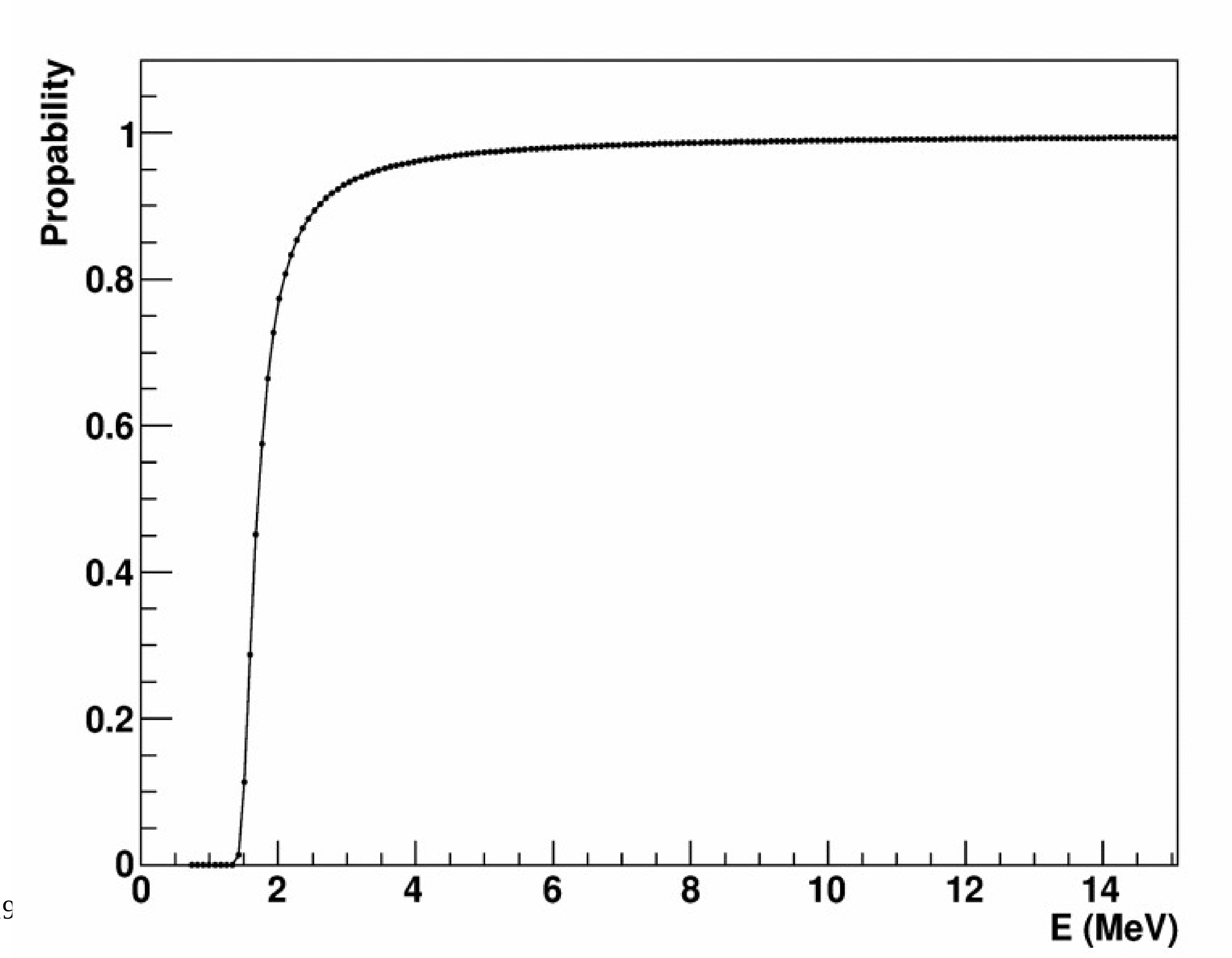

Energy to Photon Conversion

Using these values in Eq. (4), specific energy ΔE is calculated for each muon. A fraction of the energy deposited by a muon is converted into blue scintillation photons. The conversion efficiency into photons is $\sim 3\%$. These photons are emitted isotropically along the muon path. In G3sim the photon emission is quantized at every δz for ease of computation and here $\delta z = 0.1$ mm was used. The energy loss δe for δz is calculated by $\delta e = \Delta E \times \delta z$ and an equivalent number of photons N_{ph} are generated

$$N_{ph} = \frac{\delta e}{\epsilon}. \tag{5}$$

Generation of direction for Photons

ϵ = 100 eV is the energy required to produce a single photon. The photon emission is isotropic as given below,

$$\frac{dN_{ph}}{d\Omega} = \frac{N_{ph}}{4\pi}, \tag{1.6}$$

The probability of emitting a photon along θ is generated as given below and ϕ is randomly distributed from 0 to 2π,

$$P = \frac{1}{N_{ph}} \int \frac{dN_{ph}}{d\Omega} d\Omega = \frac{1}{N_{ph}} \int_0^{\theta} \int_0^{2\pi} \frac{N_{ph}}{4\pi} sin\theta \, d\theta \, d\phi = \frac{(1 - cos\theta)}{2} \tag{1.7}$$

$$\theta = cos^{-1}(1 - 2P) \tag{1.8}$$

Reflection from Scintillator Surfaces

After emission, a photon is tracked until it reaches one of the six scintillator surfaces. The coordinates of point of incidence are calculated by finding the intersection of the six planes and the photon direction as described below. General equation of a plane is,

$$ax + by + cz + d = 0 \tag{1.9}$$

The equations defining six scintillator surfaces are expressed by coefficients a, b, c, d. For top surface, z=Zmax and a=0, b=0, c=1, d=-Zmax. For the bottom surface, z=Zmin and a=0, b=0, c=1, d=-Zmin. The remaining four surfaces are similarly defined. For a photon emitted at x0, y0, z0 along θ and ϕ, its arrival at one of the surfaces defined above is calculated as follows,

$$x = x_0 + \alpha t \tag{1.10}$$

$$y = y_0 + \beta t \tag{1.11}$$

$$z = z_0 + \gamma t \tag{1.12}$$

Reflectors

Reflectors play a very significant role to enhance the light collection

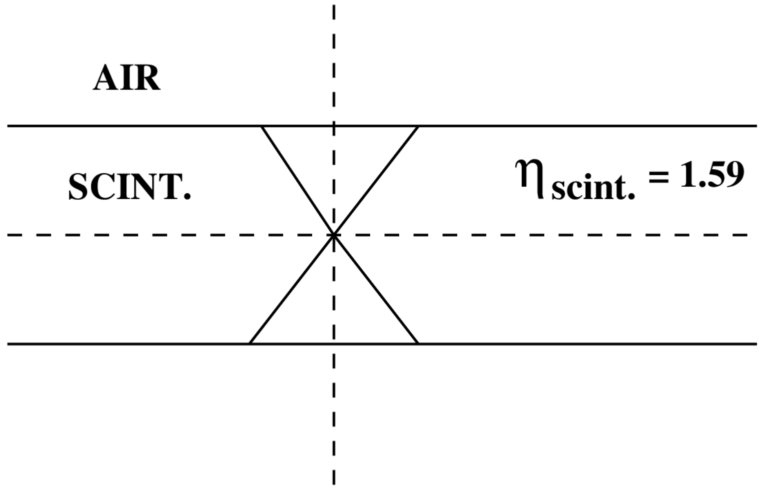

Escape fraction ~ 70%

Specular Reflection: Reflected angle is equal to incident angle ($\theta_i = \theta_r$)

Aluminum foil (Reflectivity ~ 95%)

Diffuse Reflection: Reflected angle is independent of incident angle

Tyvek has good strength and resistant to degradation (Reflectivity ~ 90%)

$$\frac{dI}{d\theta} \propto \cos\theta.$$

Reflectors

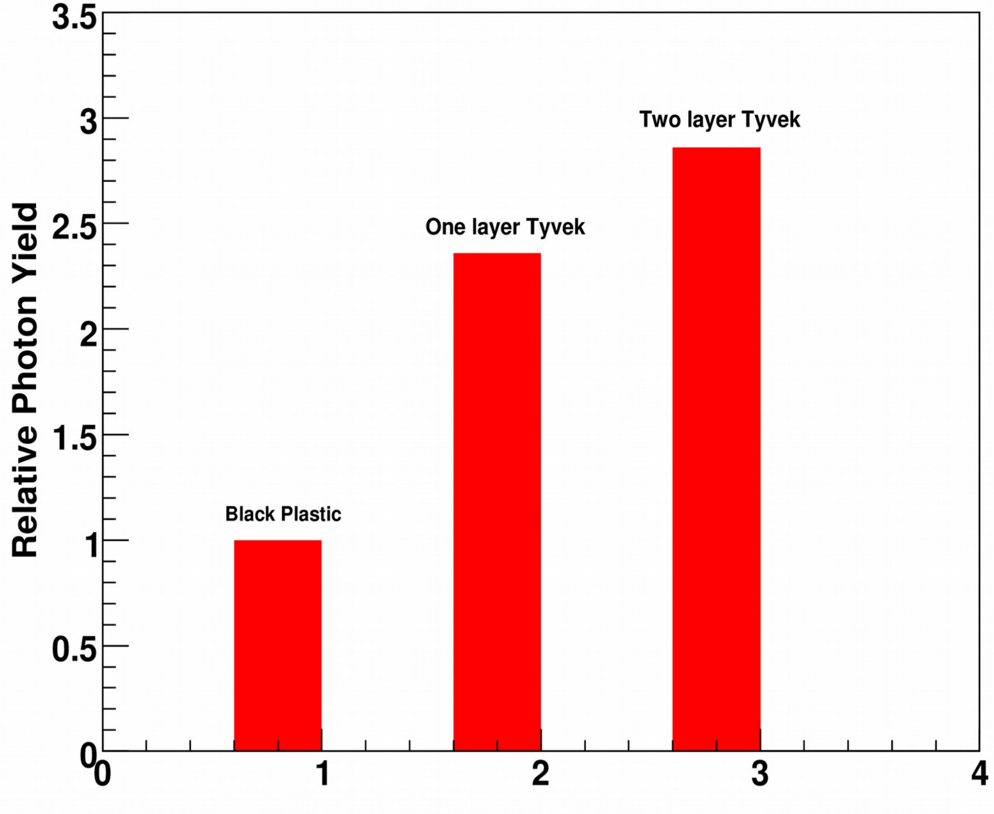

Black Plastic

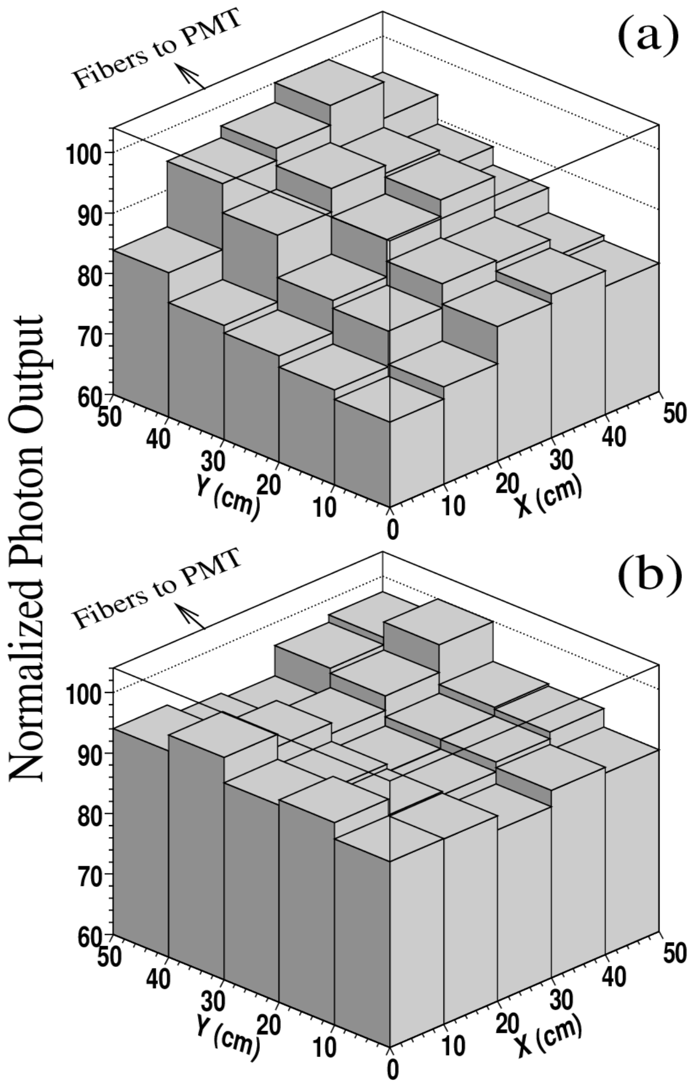

Tyvek

Light Attenuation

Self Absorption

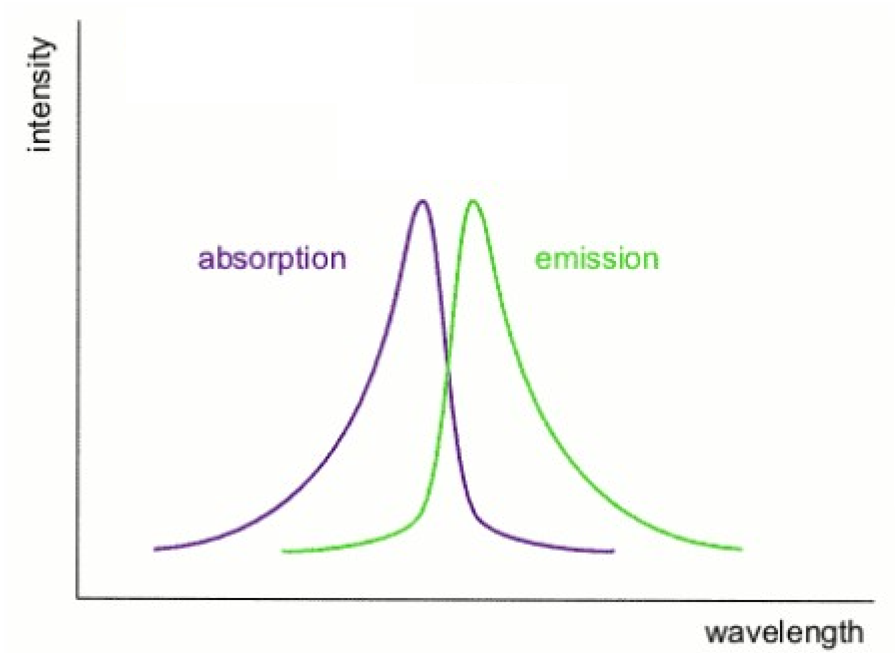

$$N(x) = N(0)e^{-x/\lambda_{sc}}$$

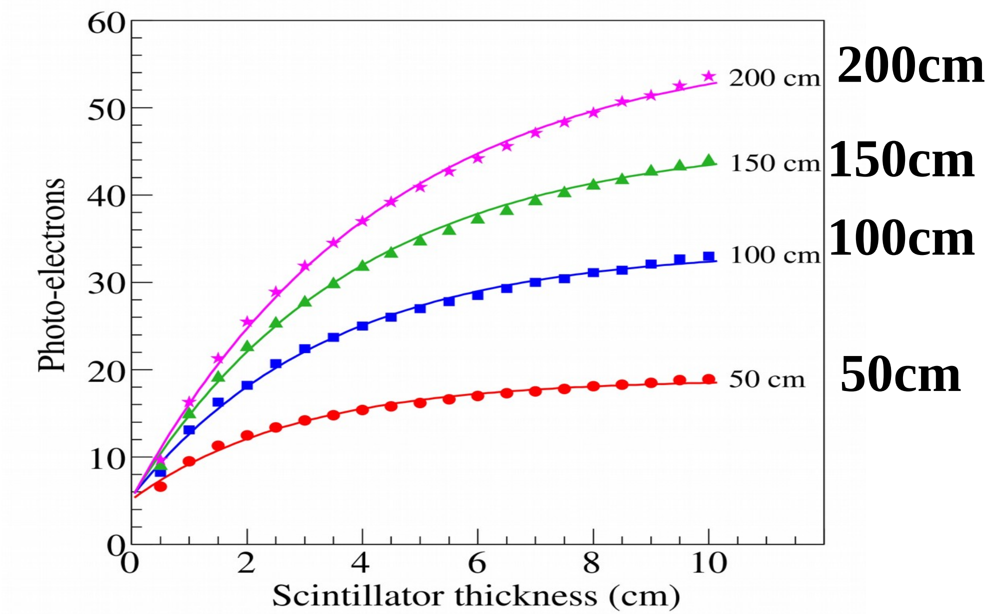

FIG. 6. Mean photo-electrons as function of thickness for λ = 50, 100, 150, 200 cm. Data fitted by PE = a - b× $e^{(-x/c)}$. Y-axis intercept a - b = (5.2 ± 0.5) and c = (3.6 ± 0.5) cm.

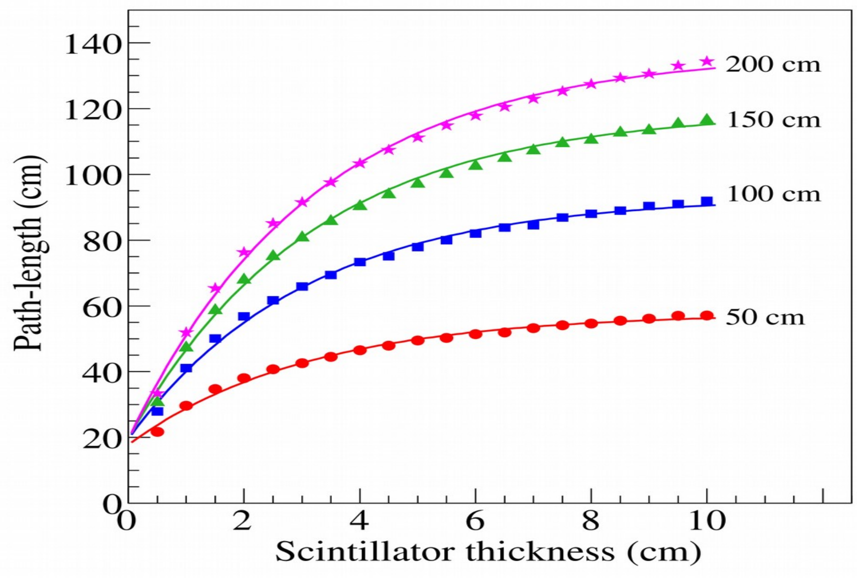

Photon Trapping in Fiber

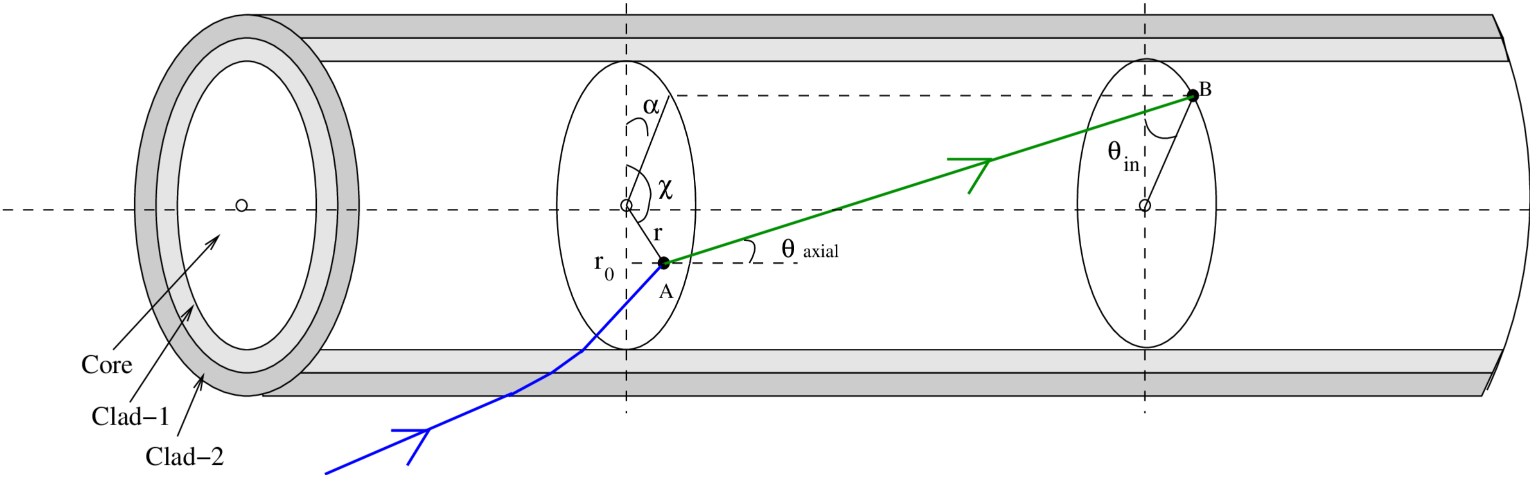

Core: 0.94mm
Refractive index = 1.59

Inner clad: 0.03mm
Refractive index = 1.49

Outer clad: 0.03mm
Refractive index = 1.42

Meridional rays

Incident, normal and reflected ray lie in the same plane

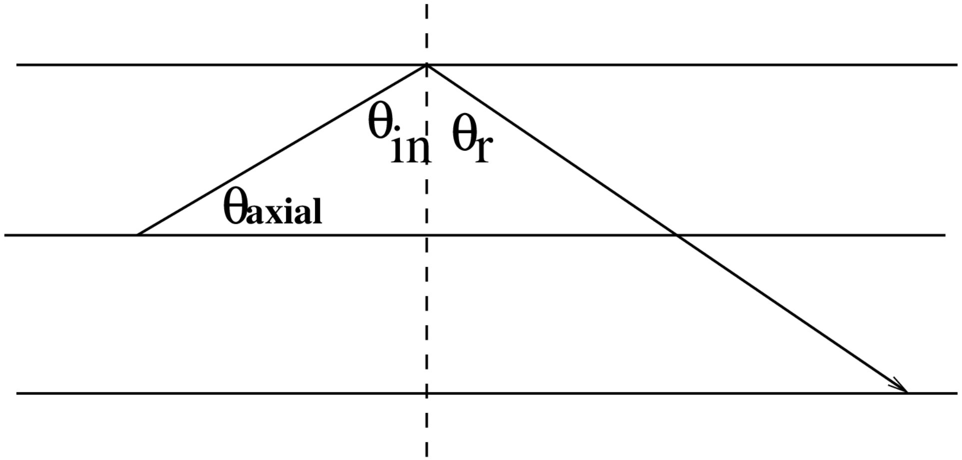

$$\cos(\theta_{in}) = \sin(\theta_{axial})$$

Skew Rays

do not lie in the same plane

$$\sin(\theta_{axial}) = \cos(\theta_{in})\left\{1 + \left(\frac{r/r_0 \sin(\chi - \alpha)}{1 - r/r_0 \cos(\chi - \alpha)}\right)^2\right\}^{1/2}$$

Ref: N.S. Kapany, Fiber Optics: Principles & Applications, Academic Press London & New York (1967)

Axial angle distribution of trapped photons

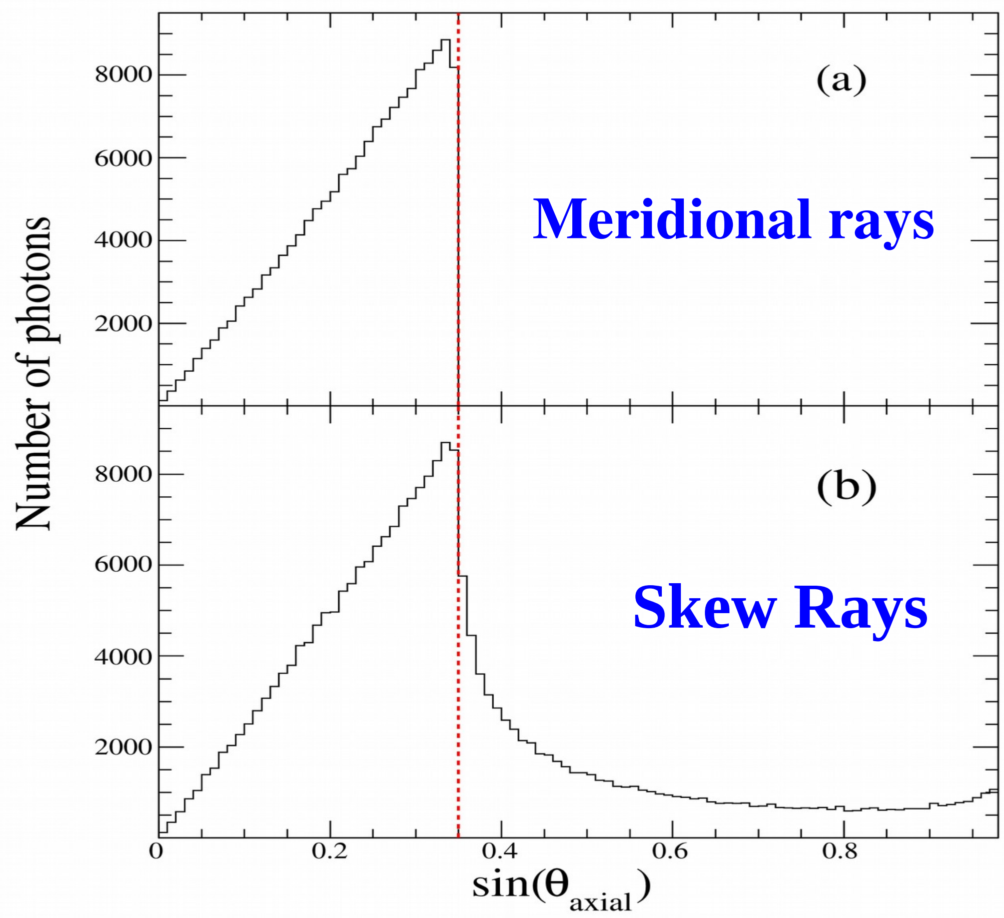

Trapping Efficiency of meridional rays = 3.2 %

With inclusion of skew rays, trapping efficiency = 4.8%

Losses in fiber

Self absorption loss : Attenuation length for Kuraray double clad fiber = 350 cm

Loss from the imperfect surface:

Total internal reflectivity $R = 0.9999$

For 1 meter long and 1mm diameter fiber, number of reflections $N \sim 500$

Survival probability = $R^N = 0.95$

Folding PMT Responses

Quantum efficiency curve

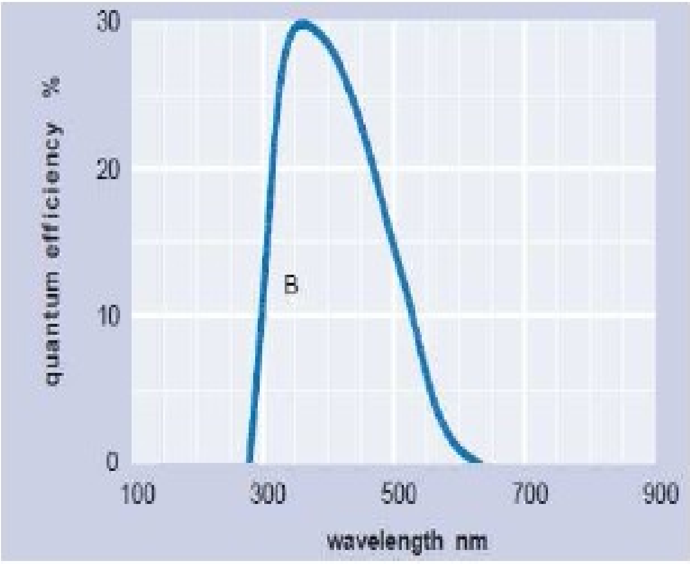

Figure 3.11: Typical quantum efficiency of an ETL PMT (model 9807B) [71].

WLS fiber emission spectrum

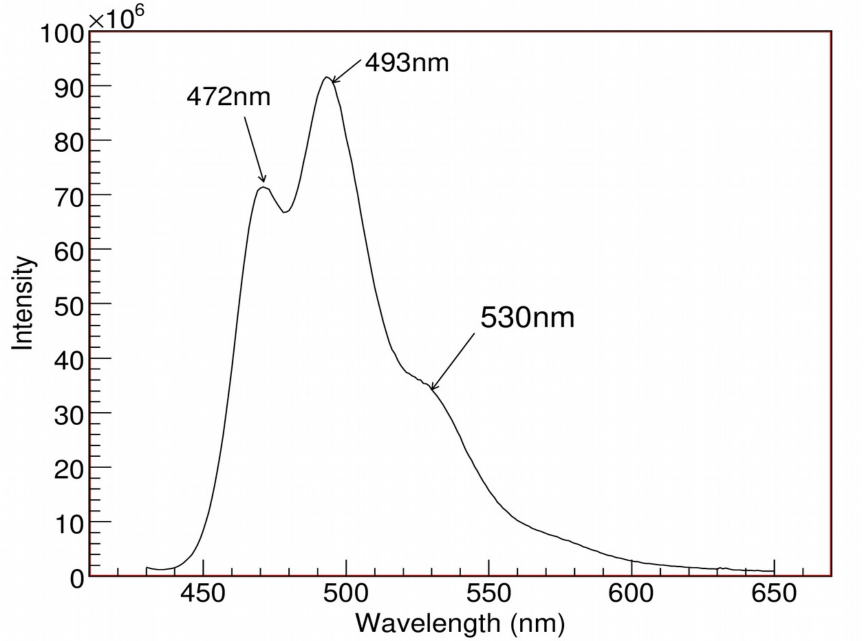

Single electron Resolution (20%) and PMT time resolution (1ns)

Input parameters

TABLE I. Simulation parameters.

Photon conversion	100 eV
Maximum reflections	150
Scintillator ETIR	0.93
Tyvek reflectivity	0.90
Fiber reflectivity	0.9999
Path-length step	0.01 cm
λ_{scint}	100 cm
λ_{WLS}	350 cm
η_{scint}	1.59
η_{core}	1.59
η_{clad-1}	1.49
η_{clad-2}	1.42
η_{air}	1.00
Min, Max (X Y Z)	−25 25 −25 25 −1 1 cm

TABLE II. Photon statistics. Photon Statistics (50 cm x 50 cm x 2cm)

Produced in scintillator	46 000	
Escaped from scintillator	11 500	
Absorbed in scintillator	30 000	
Entered WLS fiber	4500	10%
Escaped from WLS fiber	3850	
Trapped in WLS fiber	650	
Absorbed in WLS fiber	450	
Arrived at the PMT	200	0.4%

parallel **matrix** **σ**

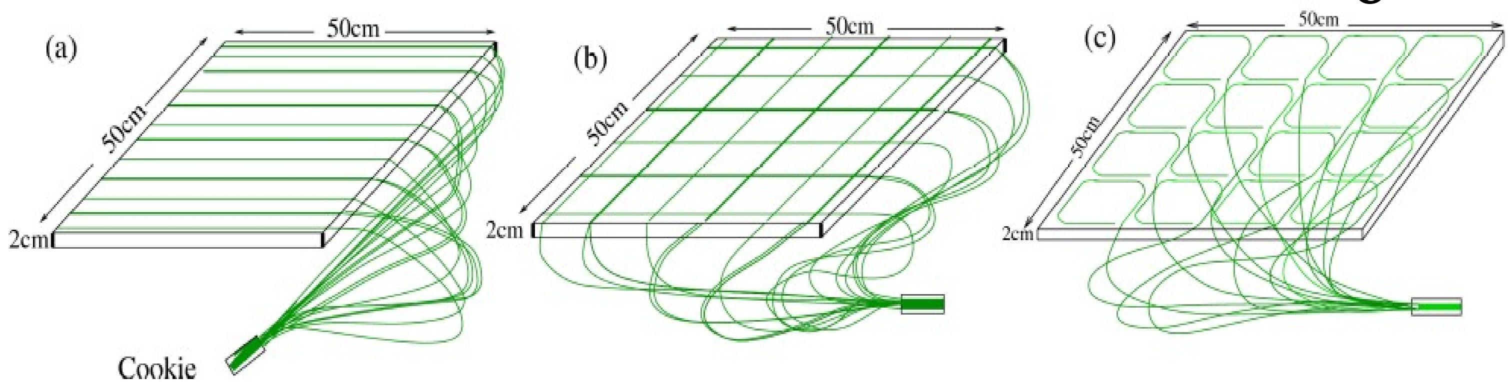

Photo-electron Yield

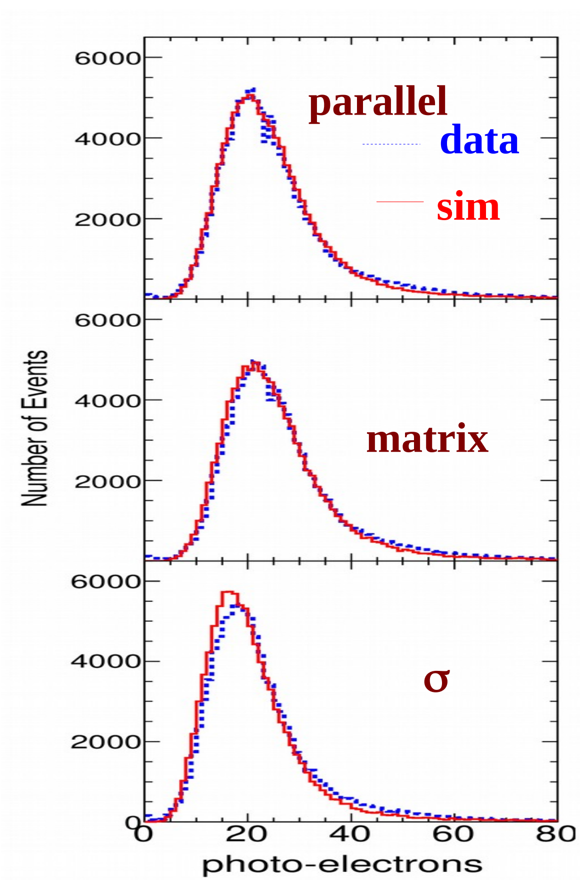

Time Response

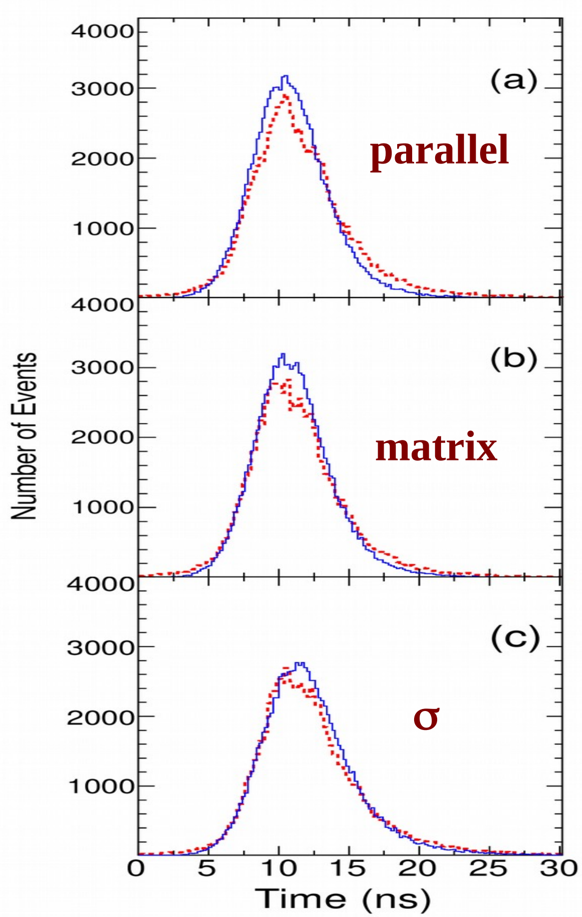

Uniformity

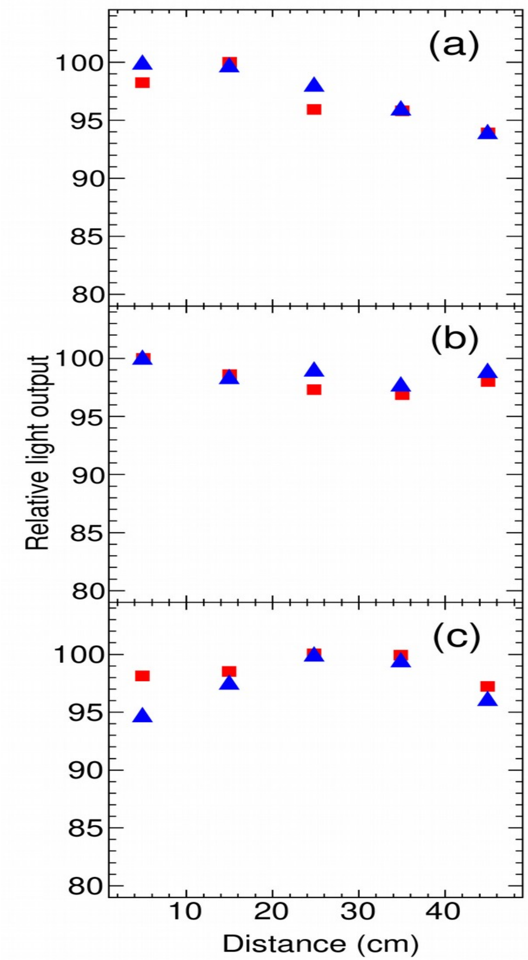

Summary of groove comparisons

Photo-electron yield

Groove	Fiber-length(cm)	Photo-electrons
Parallel	900	20.5
Matrix	900	21.7
σ	656	17.9

RMS non-uniformity (%)

Groove	Experiment	Monte Carlo
Parallel	2.7	2.0
Matrix	2.1	1.6
σ	3.5	3.3

Time Response (ns)

Groove	Experiment	Monte Carlo
Parallel	2.5	2.3
Matrix	2.4	2.3
σ	2.4	2.4

Conclusion

photo-electron yield is proportional to the length of fibers in the groove and other responses are found be independent of design.

Parallel groove design selected for final configuration because of ease in fabrication

Photon-electron with fibers

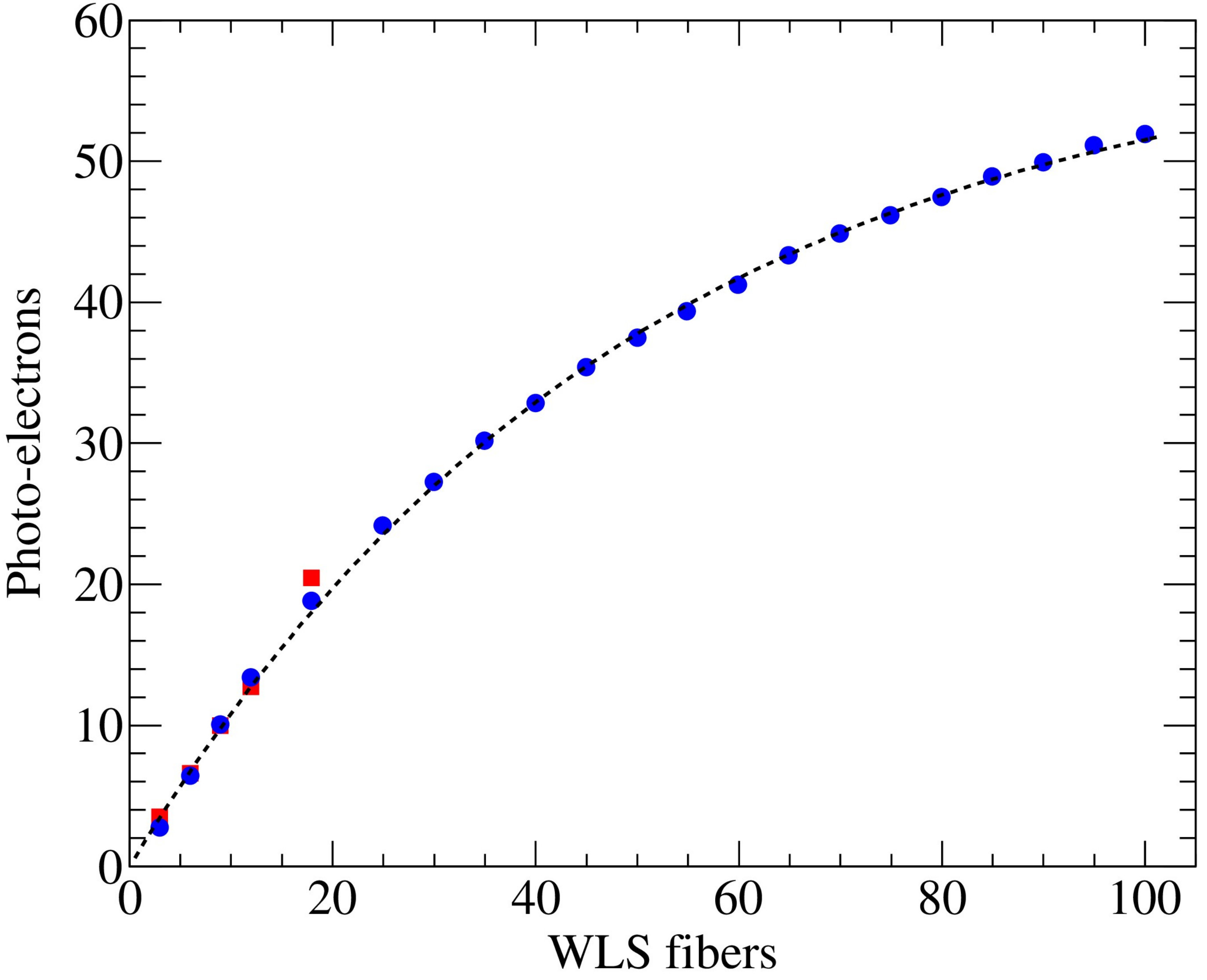

Old

New

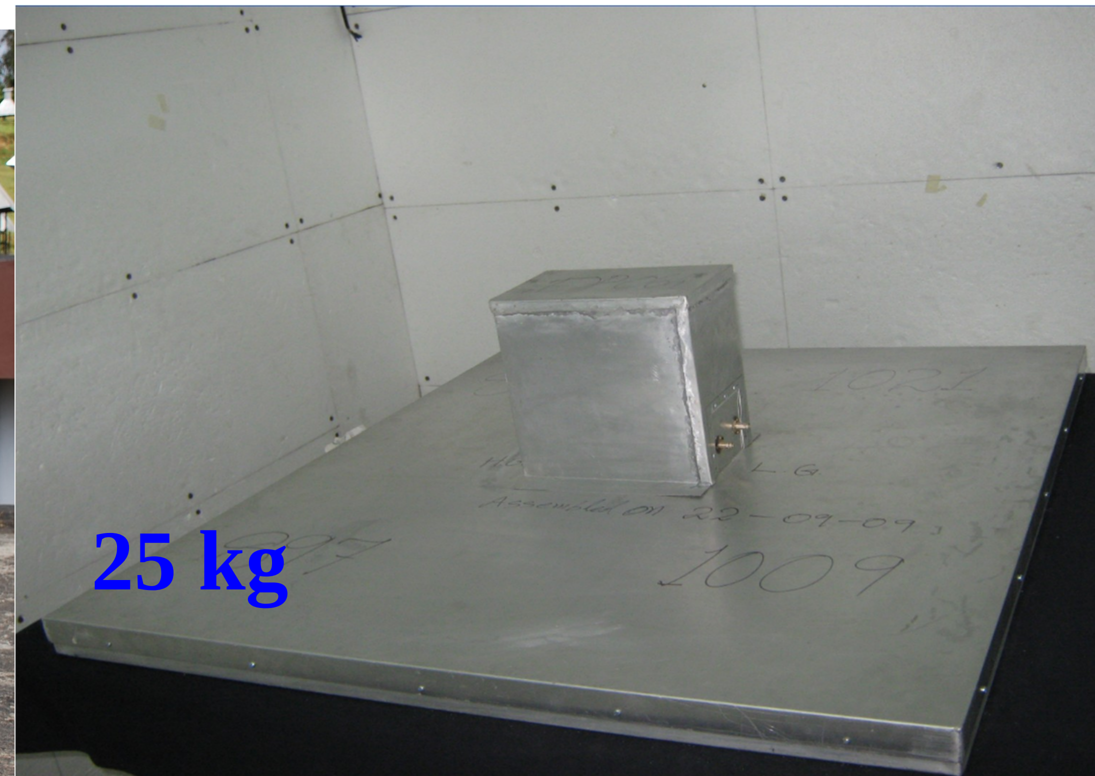

Deployment of Fiber detectors

G3sim code is available on request

(contact: pkm@tifr.res.in)

AIP | Review of Scientific Instruments

Monte Carlo code G3sim for simulation of plastic scintillator detectors with wavelength shifter fiber readout

P. K. Mohanty, S. R. Dugad, and S. K. Gupta

Citation: Rev. Sci. Instrum. **83**, 043301 (2012); doi: 10.1063/1.3698089

THANK YOU